NASA-CR-202730

Onset of strong scintillation with application to remote sensing of turbulence inner scale

Reginald J. Hill

Environmental Technology Laboratory

325 Broadway, Boulder, Colorado 80303

Rod G. Frehlich

Cooperative Institute for Research in the Environmental Sciences (CIRES)

University of Colorado, Boulder, Colorado 80309

Abstract

Numerical simulation of propagation through atmospheric turbulence of an initially spherical wave is used to calculate irradiance variance σ_I^2, variance of logirradiance $\sigma_{\ln I}^2$, and mean of logirradiance $< \ln I >$ for 13 values of l_0/R_F (i.e., of turbulence inner scale l_0 normalized by Fresnel scale R_F) and ten values of Rytov variance σ_{Rytov}^2, which is the irradiance variance, including the inner-scale effect, predicted by perturbation methods; l_0/R_F was varied from 0 to 2.5 and σ_{Rytov}^2 from 0.06 to 5.0. The irradiance probability distribution function (PDF) and, hence, σ_I^2, $\sigma_{\ln I}^2$, and $< \ln I >$ are shown to depend on only two dimensionless parameters, such as l_0/R_F and σ_{Rytov}^2. Thus, effects of the onset of strong scintillation on the three statistics are characterized completely. Excellent agreement is obtained with previous simulations that calculated σ_I^2. We find that σ_I^2, $\sigma_{\ln I}^2$, and $< \ln I >$ are larger than their weak-scintillation asymptotes (namely, σ_{Rytov}^2, σ_{Rytov}^2, and $-\sigma_{Rytov}^2/2$, respectively) for the onset of strong scintillation for all l_0/R_F. An exception is that for largest l_0/R_F, the onset of strong scintillation causes $\sigma_{\ln I}^2$ to decrease relative to its weak-scintillation limit, σ_{Rytov}^2. We determine the efficacy of each of the three statistics for measurement of l_0, taking into account the relative difficulties of measuring each statistic. We find that measuring σ_I^2 is most advantageous, although it is not the most sensitive to l_0 of the three statistics. All three statistics and, hence, the PDF become insensitive to l_0 for, roughly, $1 < \beta_0^2 < 3$ (where β_0^2 is σ_{Rytov}^2 for $l_0 = 0$); this is a condition for which retrieval of l_0 is problematic.

Key words: Turbulence, scintillation, remote sensing.

1. Introduction

We describe the variance of irradiance σ_I^2, variance of logirradiance $\sigma_{\ln I}^2$, and mean of logirradiance $< \ln I >$ for propagation through homogeneous atmospheric turbulence of an initially spherical wave. The propagation-path-averaged strength of scintillation is varied from weak to strong scintillation, and the turbulence inner scale is varied from zero to large values. The results for our three statistics are of fundamental interest, as well as of interest for remote sensing of turbulence parameters using scintillation. In particular, we are motivated by the need to extend the range of applicability of measuring turbulence inner scale using scintillation. Such measurements require simultaneous measurement of scintillation caused by two distinct bands of spatial wave numbers in the refractive-index spectrum[1]. As recently reviewed[1], these methods include measuring variance of irradiance or logirradiance from two different path lengths,[2–4] different beam types,[5] different temporal-frequency passbands,[6] the spectrum of angle of arrival for differing angles,[7,8] phase-difference structure function or covariance function at differing spacings,[9–13] beam wander,[14–17] variance of beam centroid separations for differing separations,[18] covariance of irradiance or logirradiance at different spacings,[9,19–21] the spatial spectrum of logirradiance,[22,23] spatial filtering of the irradiance pattern,[24] differing aperture sizes,[25,26] and differing radiation wavelengths.[27–31] The band at higher spatial wave numbers should be within the dissipation range of the spectrum of refractive-index fluctuations. The band at lower spatial wave numbers should be in or near the inertial-convective range. The ratio of statistics caused by these two wave-number bands provides an estimate for the inner scale: then this inner scale and either statistic give the refractive index structure parameter C_n^2.

One application of scintillation measurement of inner scale and C_n^2 using a horizontal propagation path below, say, 10 m height is the determination of the fluxes of heat and momentum between the surface and the atmosphere. These fluxes, along with the humidity flux, are the basic interaction between the surface and the atmosphere. Hill[1] reviewed the methods and the practice of scintillation measurements of surface fluxes. Extending the range of measurements of inner scale and C_n^2 also extends the range of surface-flux determination.

Here, we consider in detail a scintillometer for measuring inner scale and C_n^2 as described by Ochs and Hill.[26] The band of higher spatial wave numbers is obtained by using a diverged laser beam to emulate a spherical wave and a small aperture to emulate a point receiver. The band of lower spatial wave numbers is obtained by transmitting phase-incoherent radiation that uniformly illuminates a large, circular transmitter aperture and by receiving the scintillating radiation through a circular aperture of the same diameter. One version of this inner-scale scintillometer uses logarithmic amplifiers to produce logirradiance variance for both the laser and large-aperture channels. Another version uses linear amplifiers to produce irradiance variance from both channels. For either type of large-aperture variance, the theory by Frehlich and Ochs[32] gave the variance as a function of inner scale and C_n^2 (in terms of dimensionless parameters). Using this theory, the variance from the large aperture is used as part of the information needed for remote sensing of inner scale. The theory of Frehlich and Ochs[32] includes both the effect of inner scale as well as the effect of strong scintillation on the large-aperture variance. Their theory is thus more general than the theory by Hill and Ochs[25] (which was previously used for retrieval of l_0 and C_n^2) and reduces to the theory in Ref. 25 in the limit of weak scintillation.

However, until recently, there has been no calculation of the variances of irradiance or logirradiance for a spherical wave that includes the transition from weak to strong scintillation. This calculation is needed to extend the range of operation of the inner-scale scintillometer and to more precisely obtain inner scale. Indeed, the variance of the laser radiation is significantly more sensitive to effects of strong scintillation than is the large-aperture variance: this is well known from the theory of aperture averaging.[32–34]

We use numerical simulation to calculate our three statistics. Simulations of wave propagation through three-dimensional random media with narrow angular scattering (parabolic equation approximation) have been used in various investigations.[35–41] A simulation consists of approximating a three-dimensional random medium as a collection of equally spaced, two-dimensional, random phase screens that are transverse to the direction of wave propagation. The wave is propagated through the collection of phase screens using Fresnel diffraction theory in Fourier transform representation. This is efficiently performed with a two-dimensional fast Fourier transform. These simulations are demanding of computational resources, and careful choice of numerical parameters is essential for valid results. Quantitative results for the optimal choice of the mesh size and screen separation for simulation of wave propagation through a three-dimensional random medium have been determined for plane- and spherical-wave geometry. We use the spherical-wave algorithm described by Coles *et al.*[42]

The assumptions used to obtain field-moment equations are narrow-angle scattering (hence, use of the parabolic wave equation), the Markov approximation, and the approximation of Gaussian refractive index. The refractive-index spectrum must be specified along the propagation path. The same assumptions are used in simulation of propagation. Both simulation and field-moment methods have the same range of validity. As one of us had noted previously,[43] the quantitative agreement of simulations with scintillation experiments validates both simulation as well as fourth-order field-moment methods.

The validity of the Markov approximation was first investigated by assuming a Gaussian random process for the refractive index fluctuations with a correlation distance that is much smaller than the length of the propagation path (the Markov property).[44,45] These assumptions are not as restrictive as they appear. Validity of moment equations has been established on the basis of weaker approximations.[46,47] Zavorotny[48] obtained conditions for the validity of field-moment equations of all orders by considering the irradiance moments of all orders for both very weak and very strong scintillation. He determined that the wavelength must be much smaller than both the Fresnel scale and the wave coherence length and that the propagation path length must be very much greater than both the Fresnel scale and size of the scattering disk. These conditions are easily satisfied for atmospheric propagation.

2. Propagation Parameterization

We define the following parameters: λ is the wavelength of the radiation: L is the length of the propagation path: z is the position along the path from $z = 0$ at the transmitter to $z = L$ at the receiver: $R_F = \sqrt{L/k}$ is the Fresnel distance; C_n^2 is the refractive-index structure parameter: and l_0 is the inner scale of turbulence. We use Obukhov's[49] definition of inner scale: this definition is also given in Tatarskii's[50] Sec. 13, as well as given by Hill and Clifford.[51] Briefly, the inner scale is the spacing at which the asymptotic formula for the inertial-convective range of the refractive-index structure function equals its asymptotic dissipation-range formula.

We denote irradiance normalized by its mean value by I and use angle brackets to denote an ensemble average. Thus, $< I >= 1$. The three statistics we study are

$$\text{irradiance variance}, \ \sigma_I^2 =< (I-1)^2 > , \tag{1a}$$

$$\text{mean of logirradiance} \ , \ < \ln I > , \tag{1b}$$

$$\text{variance of logirradiance} \ , \ \sigma_{\ln I}^2 =< (\ln I - < \ln I >)^2 > \ . \tag{1c}$$

Note that (1a and 1b) require a measurement of mean irradiance in order to determine the normalized irradiance I. However, (1c) does not require measurement of mean irradiance because, if S is any scaling factor, then $\ln(SI) - < \ln(SI) >= \ln I - < \ln I >$.

We call the irradiance variance in the weak-scintillation limit the Rytov variance and denote it by σ_{Rytov}^2. In this limit of very weak scintillation, we have[50]

$$\sigma_{Rytov}^2 = \sigma_I^2 = \sigma_{\ln I}^2 = -2 < \ln I > \ . \tag{2}$$

For isotropic turbulence, the refractive-index spectrum $\Phi_n(\kappa)$ can be written as the product of the inertial-range formula and a dimensionless function $f(\kappa l_0)$, where κ is the spatial wave number, i.e.,

$$\Phi_n(\kappa) = 0.033 C_n^2 \kappa^{-11/3} f(\kappa l_0) . \tag{3}$$

The dimensionless function $f(\kappa l_0)$ describes the spectral bump and dissipation range at high wave numbers, and $f(0) = 1$. $f(\kappa l_0)$ depends only on the dimensionless variable κl_0. A theoretical model for $\Phi_n(\kappa)$, and therefore for $f(\kappa l_0)$, is given by Hill,[52] who showed that the model fits data from precision thermometry in atmospheric turbulence to within the accuracy of the data. The function $f(\kappa l_0)$ from this model is shown in figures in Refs. 35, 41, 51, 28, 30, 31 and need not be shown here.

Geophysical flows have variability (sometimes called global intermittency[53]) on spatial scales that greatly exceed the propagation path length, as well as on scales commensurate with the path length. The corresponding temporal scales greatly exceed those caused by the wind advecting those refractive-index fluctuations that are in the range of spatial scales producing scintillation. From a propagation point of view, such variability means that C_n^2 and l_0, or equivalently, the dissipation rates of energy and of refractive-index variance, must be treated as locally stationary with intermittent values.

Hill[54] and Frehlich[21] presented equivalent models of the effects of global intermittency of C_n^2 and l_0 on the refractive-index spectrum. They showed that global intermittency causes variability in the shape of $f(\kappa l_0)$. Such variability has been observed[21]. The effects of global intermittency have been observed in short-path measurements of irradiance PDF[55] and irradiance covariance[20]. Intermittency effects on propagation are further discussed in Refs. 56–59. We assume that the intermittency in C_n^2 and l_0 is stationary in time and homogeneous along the propagation path and that the average spectrum is given by (3) with $f(\kappa l_0)$ as given in Ref. 52. If the variability of C_n^2 and l_0 due to global intermittency produces significant deviations from the assumed universal function $f(\kappa l_0)$, then estimates of inner scale will have a bias.

Atmospheric scintillation experiments have shown that Eq. (3) with $f(\kappa l_0)$ as given in Ref. 52 must be used to quantitatively predict weak scintillation.[21,25,26,28,31,60] These experimental results are reviewed in Ref. 1. Recently, experiment[43] and numerical simulation[35] have shown that this model for $\Phi_n(\kappa)$ is necessary to quantitatively predict strong scintillation from atmospheric propagation. Flatté *et al.*[35] noted that the agreement of the irradiance variance obtained from numerical simulations with that obtained by experiment, as well as with other theoretical calculations, gives confidence in the use of numerical simulation for quantitative prediction of atmospheric scintillation.

Formulas for σ^2_{Rytov} in terms of $\Phi_n(\kappa)$ for a spherical wave propagating through isotropic turbulence that is homogeneous along the propagation path are given, for instance, by equations (T8) and (T26) of Lawrence and Strohbehn.[61] Let $x = \kappa R_F$ be the dimensionless wave number, and let $u = z/L$ be the dimensionless propagation path position. Substituting (3) into (T26) of Lawrence and Strohbehn[61] and changing integration variables gives

$$\sigma^2_{Rytov} = \beta_0^2 \tilde{\sigma}^2(l_0/R_F) \tag{4}$$

where

$$\beta_0^2 = 0.496 k^{7/6} L^{11/6} C_n^2 \tag{5}$$

and

$$\tilde{\sigma}^2(l_0/R_F) = 10.5 \int_0^1 du \int_0^\infty dx x^{-8/3} f(x l_0/R_F) \sin^2[x^2 u(1-u)/2] \tag{6}$$

The quantity β_0^2 in (5) is the weak-scintillation variance for an inertial range extending over all wave numbers (i.e., for $l_0 = 0$). Thus, $\tilde{\sigma}^2(0) = 1$. The dimensionless function $\tilde{\sigma}^2(l_0/R_F)$, as defined in Eq. (6), is manifestly a function of only its one dimensionless argument. Thus, $\tilde{\sigma}^2(l_0/R_F)$ gives the effect of the spectral bump and dissipation range of $\Phi_n(\kappa)$: in other words, it gives the inner-scale effect. Based on the form of $f(\kappa l_0)$ discussed previously, Fig. 3 in Ref. 30 shows $\tilde{\sigma}^2(l_0/R_F)$ as a function of its sole dimensionless argument; Fig. 4 in Ref. 51 and Fig. 2 in Ref. 31 show $\tilde{\sigma}^2$ as a function of $\sqrt{\lambda L/l_0} = \sqrt{2\pi}(l_0/R_F)^{-1}$.

The dimensionless quantities σ^2_{Rytov} and l_0/R_F are used to present our results for the three statistics of interest. We also present results in terms of the dimensionless quantities β_0^2 and

l_0/R_F. We next show that only two dimensionless parameters are needed to determine the irradiance and logirradiance statistics for our case.

We consider the case of a spherical wave propagating in homogeneous atmospheric turbulence having an outer scale much larger than the spatial sizes of refractive-index fluctuations that cause irradiance scintillations. In this case, the turbulence imparts to the propagation statistics of interest a dependence on the parameters C_n^2 and l_0. The statistics also depend on k and L. However, the statistics depend on only two dimensionless parameters.

For plane waves in a homogeneous random medium having a Kolmogorov power-law refractive-index spectrum (i.e., $l_0 = 0$), Gracheva *et al.*[62] obtained that the probability distribution function (PDF) of the irradiance depends on only one parameter. This parameter can be taken to be β_0^2. Gracheva *et al.*[62] obtained this result by expressing the field-moment equations (cf., Ref. 50) of all orders in terms of dimensionless independent variables. This method reveals the dependence of the field moments on the minimum number of dimensionless parameters and dimensionless independent variables. Single-point moments of all orders of the irradiance are special cases of the field moments and are thereby shown to depend on a minimum number of dimensionless parameters. For the specific case of the fourth-order moment of the field, Tatarskii[44], Gurvich and Tatarskii[63], and Gurvich et al.[64] show that a nonzero inner scale results in one additional dimensionless parameter to be relevant. This parameter may be taken to be l_0/R_F.

We extend the method of Gracheva *et al.*[62] to spherical waves by use of a spherical coordinate system and, for that matter, to cylindrical waves using a cylindrical coordinate system. Moreover, as noted in Gracheva *et al.*,[62] the case of beamed waves requires as many more dimensionless parameters as there are parameters describing the initial beam, such as initial beam width and focal length. In addition, we generalize the method of Ref. 62 to refractive-index spectra that have more parameters, such as inner and outer scales or a scale demarking a transition between two power-law regimes (this latter case is studied in Refs. 64–66). The result is that the field moments and, hence, the single-point irradiance moments and, hence, irradiance PDF depend on one additional dimensionless parameter for each such parameter of the refractive-index spectrum. For our case, we take the outer scale to be so large that irradiance statistics have negligible dependence on outer scale. Therefore, we obtain that the irradiance PDF depends on only two dimensionless parameters: one can be taken to be σ^2_{Rytov}, and the other can be l_0/R_F. Thus, any irradiance statistic obtainable from the irradiance PDF can be taken to depend only on these two dimensionless parameters; in our study, this applies to σ^2_I, $\sigma^2_{\ln I}$, and $< \ln I >$. As stated in the introduction, the demonstrated dependence on only a minimum number of dimensionless parameters depends on the validity of the field-moment equations.

In addition, for the case of inhomogeneous turbulence, we can also obviously allow the parameters of turbulence [e.g., C_n^2, l_0, and even the functional form of $f(\kappa l_0)$] to vary slowly along the propagation path. To do so, the scattering function within the equation for a field moment of arbitrary order is taken to be a functional of the distribution of the parameters in question [e.g., C_n^2, l_0, $f(\kappa l_0)$] rendered dimensionless by scaling with their propagation-path-averaged values and expressed in terms of the dimensionless propagation position z/L. Then arbitrary field moments, and hence the irradiance PDF, are functionals of the dimensionless path distribution of the turbulence parameters. Tatarskii[44] derived an equation of the Fokker-Planck type for the characteristic functional of the field. From this equation, one can generate the field-moment equations of all orders. It is clear that the demonstration of dependence of field statistics on a minimum number of dimensionless parameters and dimensionless path distributions of turbulence parameters can be obtained by introducing scaled variables and a dimensionless scattering function into Tatarskii's equation for the characteristic functional of the field.

3. Basic Results

Previous simulations of spherical-wave propagation in three-dimensional random media used a Cartesian coordinate system with a small Gaussian source distribution[36,39] or a small circular disk.[41] Those simulations produce an average irradiance that varies with location on the observation plane, as well as numerical artifacts near the edge of the simulation. An alternative method is to compute the random field using a spherical coordinate system.[42] This method produces a constant average irradiance in the observation plane with no numerical artifacts.[42] Coles *et al.*[42] obtained error scaling using simulations with varying grid sizes and screen. The spherical coordinate system is numerically much more efficient than the Cartesian coordinate system.

The results presented here use 512x512 grid points per phase screen with 20 screens along the propagation path per realization; 50 realizations were averaged to produce our statistics for each l_0/R_F and σ^2_{Rytov}. The Fresnel distance was 10 grid points. The numerical errors for the normalized irradiance variance were less than 2% for all cases and are not plotted on our figures because they would be hardly noticeable.

Figure 1a shows σ^2_I as a function of Rytov variance σ^2_{Rytov}; a straight line indicates $\sigma^2_I = \sigma^2_{Rytov}$. The onset of strong scintillation causes σ^2_I to exceed σ^2_{Rytov}, and the greater l_0/R_F is, the more σ^2_I exceeds σ^2_{Rytov}. Of course, it is well known that σ^2_I attains a maximum as σ^2_{Rytov} increases further and that σ^2_I approaches unity as σ^2_{Rytov} tends to infinity.[62,67–71] As shown in Fig. 1b, the maximum occurs beyond the range of our abscissa in Fig. 1a. Tur[72] showed a case, very different from ours, for which σ^2_I exceeds σ^2_{Rytov} at the onset of strong scintillation. Tur solved the fourth-moment equation for a Gaussian refractive-index spectrum in two-dimensional space.

The legend for l_0/R_F in Fig. 1a is in the order of the curves from top to bottom. We see from the curves and legend that as l_0/R_F increases from zero, the value of σ^2_I at first decreases (for fixed σ^2_{Rytov}) until $l_0/R_F \approx 0.12$, and then σ^2_I increases (for fixed σ^2_{Rytov}) as l_0/R_F increases further. This latter effect is attributable to the bump in the refractive-index spectrum and the same effect in the behavior of the heuristic theory of logamplitude variance (cf., Fig. 8 in Ref. 73) is caused by the bump in the refractive-index spectrum. In fact, the motivation for graphing σ^2_I versus σ^2_{Rytov} is the orderly progression of the curves that was anticipated on the basis of the heuristic theory.

Figure 1a shows that σ_I^2 approaches σ_{Rytov}^2 as σ_{Rytov}^2 becomes small, as it should. For a fixed value of σ_{Rytov}^2 less than about unity, Fig. 1a shows that σ_I^2 deviates more from σ_{Rytov}^2 for larger l_0/R_F. This is not necessarily the case for fixed β_0^2, as opposed to fixed σ_{Rytov}^2 (cf., Ref. 41).

Figure 1b shows σ_I^2 from our simulations compared with σ_I^2 from the simulations by Flatté *et al.*[35] Their simulations extend to greater values of σ_{Rytov}^2 (and β_0^2) than do ours. Their simulations have greater statistical uncertainty than do ours; this can be seen from the error bars shown by Flatté *et al.*[35] Considering their statistical uncertainty, the agreement between the two simulations, as shown in Fig. 1b, is excellent. Figure 1b shows the maximum of σ_I^2 and the subsequent decrease of σ_I^2 with further increase of σ_{Rytov}^2.

Figure 2 shows $\sigma_{\ln I}^2$ versus σ_{Rytov}^2; a straight line indicates $\sigma_{\ln I}^2 = \sigma_{Rytov}^2$. There are fewer curves in Fig. 2 as compared with Fig. 1b simply to reduce the crowding of the curves in Fig. 2. We see that if $l_0/R_F < 1.3$, then the onset of strong scintillation causes $\sigma_{\ln I}^2$ to initially exceed σ_{Rytov}^2, whereas if $l_0/R_F > 1.3$, then $\sigma_{\ln I}^2$ is less than σ_{Rytov}^2. For $l_0/R_F = 1.3$, $\sigma_{\ln I}^2$ is nearly equal to σ_{Rytov}^2 over the greatest range of σ_{Rytov}^2. Of course, as $\sigma_{Rytov}^2 \rightarrow \infty$, then $\sigma_{\ln I}^2 \rightarrow \simeq 1.64$. Beginning with $l_0/R_F = 0$ on the right edge of Fig. 2, we see that $\sigma_{\ln I}^2$ initially decreases slightly as l_0/R_F increases (until $l_0/R_F = 0.12$); thereafter, $\sigma_{\ln I}^2$ increases with further increases of l_0/R_F. The initial decrease of $\sigma_{\ln I}^2$ at the right edge of Fig. 2 is caused by the bump in the refractive-index spectrum. Note that the curve for $l_0/R_F = 2.5$ has not yet crossed the curve for $l_0/R_F = 1.3$ at our largest σ_{Rytov}^2. Of course, $\sigma_{\ln I}^2$ approaches σ_{Rytov}^2 in Fig. 2 as σ_{Rytov}^2 becomes small. The behavior of $\sigma_{\ln I}^2$ in Fig. 2 differs from that predicted by the heuristic theory originated by Clifford *et al.*[74] and later refined.[73,75] The heuristic theory curves shown in Fig. 8 of Ref. 73 all lie below the straight line (i.e., the heuristic theory gives $\sigma_{\ln I}^2 < \sigma_{Rytov}^2$ for all l_0/R_F), and those curves progressively approach the straight line as l_0/R_F increases. In the Appendix, we quantitatively compare the results of our simulations with the heuristic theory.

Figure 3 shows $< \ln I >$ versus σ_{Rytov}^2. The solid curve in Fig. 3 shows the weak-scintillation limit $< \ln I > = -\sigma^2_{Rytov}/2$, and the curves all approach this limit as σ^2_{Rytov} decreases. The onset of strong scintillation causes $< \ln I >$ to be larger than the weak-scintillation limit. From top to bottom, the curves in Fig. 3 are in the same order as the values of l_0/R_F in the legend. For smaller l_0/R_F in Fig. 3, one sees that $< \ln I >$ increases more with increasing σ^2_{Rytov} with the exception of the reverse trend for curves $l_0/R_F = 0.0$ and 0.12. This reverse trend is caused by the bump in the refractive-index spectrum, just as for our other statistics σ_I^2 and $\sigma^2_{\ln I}$. As $\sigma^2_{Rytov} \to \infty$, $< \ln I > \to -\gamma \simeq -0.577$, where γ is Euler's constant.[76] This is derived from the fact that the PDF of irradiance is exponential in this limit.

We have compared our simulations with available measurements of $\sigma^2_{\ln I}$ and σ_I^2. In all cases, the comparisons reveal limitations in the method of measuring C_n^2 and, in most cases, the limitation caused by the absence of measurement of inner scale. Ochs[77] obtained data for $\sigma^2_{\ln I}$ and obtained C_n^2 from fine-wire thermometry; he also measured wind speed. Hill and Clifford[74] used the wind speed to determine inner scale and thereby compared the heuristic theory with the data by Ochs.[77] We have performed a similar comparison with the result that our values of $\sigma^2_{\ln I}$ are somewhat in better agreement with the data by Ochs than is the heuristic theory. However, Ochs[77] obtained inconsistent values of C_n^2 from fine-wire thermometers used simultaneously at different spacings. The resulting uncertainty in the value of C_n^2, as well as the scatter in his plotted values, prevents a useful quantitative comparison with our simulations. Parry and Pusey[78] and Parry[79] measured σ_I^2 on a variety of propagation path lengths. They simultaneously obtained C_n^2 from short-path laser-irradiance variance assuming that $l_0 = 0$. Their assumption that $l_0 = 0$ is likely to produce an underestimate of C_n^2 (cf., Ref. 51), but it could also produce an overestimate of C_n^2.[51] Our comparison with their data shows an underestimate of C_n^2 of the expected magnitude. Phillips and Andrews[80] used the same method of determining C_n^2 as did Refs. 78 and 79, and their data are less explicable, perhaps because of the mirage effect discussed in Ref. 81. Coles and Frehlich[8] obtained five values of σ_I^2 that are within the range of our simulations. They obtained C_n^2 from focal-spot spread using a telescope and photographic film. Their four cases of weakest scintillation, for which $\sigma_I^2 < 1.0$, were obtained late at night during periods of very little wind. Such periods are characterized by intermittent bursts of turbulence separated by laminar flow containing strong temperature gradients that cause extreme beam wander. Indeed, such beam wander was observed, and it had the effect of causing overestimation of C_n^2. This explains why their four cases of weakest scintillation (shown in Fig. 12 of Ref. 8) correspond to C_n^2 values that are substantially too large for agreement with either weak-scintillation theory or our simulations. This illustrates the problem of attempting to measure atmospheric weak scintillation using long and low propagation paths; shorter and/or higher paths are needed. The datum of Coles and Frehlich[8] for which $\sigma_I^2 = 3.3$ was obtained in more homogeneous turbulence. This datum is in very good agreement with our simulations provided that the inner scale was less than 1 cm, which was very likely the case.

Consortini *et al.*[43] used an optical-scintillation crosswind instrument to obtain C_n^2 and crosswind. This instrument is not optimized to determine C_n^2 and can overestimate C_n^2, although this instrument has negligible inner-scale effect. As discussed by Consortini *et al.*[43], the digitization rate used for their C_n^2 signal causes scatter in their measured C_n^2. Our comparison with their data shows both such overestimation and scatter in their measured C_n^2. Flatté *et al.*[35] compared simulation with the data in Ref. 43 for cases of large β_0. Their comparison is insensitive to errors in C_n^2 because σ_I^2 varies slowly with β_0, and thereby with C_n^2, for cases of large β_0. Also, the experiment in Ref. 43 used relatively long and low propagation paths in order to measure σ_I^2 for large β_0. They show that their observed cases of smaller β_0, with which we must compare, correspond to temporally nonstationary data. We conclude that the precision and detail with which numerical simulation predicts irradiance statistics place very stringent demands on experimental measurements of C_n^2 that have not yet been attained (with the exception of one datum in Ref. 8) but that are within technological limitations.

4. Implications for Inner-Scale Scintillometry

Next we consider the efficacy of each of our three statistics for purposes of retrieval of a value of inner scale for various values of l_0/R_F and strength of scintillation. To do so, we must separate the dependence on strength of scintillation from the dependence on l_0/R_F. We choose β_0 as our strength-of-scintillation parameter because $\beta_0^2 \propto C_n^2$, β_0 is independent of l_0/R_F, and β_0 is a dimensionless parameter that provides applicability of the results to any experiment independent of the other dimensional parameters (e.g., k, L, and C_n^2). Graphing scintillation statistics versus β_0 rather than β_0^2 produces a clearer display for small β_0.

The method of obtaining inner scale from scintillometers of the type devised by Ochs and Hill[26] is to divide the laser-propagation statistic (e.g., $\sigma_{\ln I}^2$ or σ_I^2, etc.) by the variance from a large-aperture scintillation measurement. The purpose of this division is to remove the proportionality to C_n^2 of the laser-propagation statistic such that the resulting ratio depends only on l_0/R_F (in the weak-scintillation limit). The large-aperture diameter D is chosen to be much larger than l_0 such that the large-aperture variance has only a slight dependence on l_0/D (cf., Ref. 25). Ignoring this slight l_0-dependence, the large-aperture variance is proportional to β_0^2; the proportionality constant is dimensionless and does not affect the universal applicability of our results. For our purposes, it suffices to present our statistics divided by β_0^2; this removes, in a universal and dimensionless manner, a factor of C_n^2 from our statistics. Of course, the resulting ratios, i.e., σ_I^2/β_0^2, $\sigma_{\ln I}^2/\beta_0^2$, and $< \ln I >/\beta_0^2$, have increasing dependence on β_0^2 (i.e., on C_n^2) as scintillation strength increases beyond the weak scintillation case. These ratios are close approximations to the ratios of laser-radiation statistics to large-aperture variance obtainable from the inner-scale scintillometer.

In Figs. 4a,b,c, the respective ratios σ_I^2/β_0^2, $\sigma_{\ln I}^2/\beta_0^2$, and $-2 < \ln I > /\beta_0^2$ are shown versus β_0 for the values of l_0/R_F given in the legends. Because our data are calculated at the same values of σ_{Rytov}^2 for all values of l_0/R_F, the curves in Figs. 4a,b,c, begin and end at various β_0. The effect of increasing strength of scintillation on the three ratios is seen as β_0 increases along the abscissas of Figs. 4a,b,c. The ratios decrease rapidly for the larger values of β_0, and in Figs. 4a and 4b there is typically a slow increase of the ratios prior to this rapid decrease as β_0 increases. From top to bottom, the legends give the values of l_0/R_F corresponding to the curves' top-to-bottom position along the left side of Figs. 4a,b,c. The short-dashed curves for $l_0/R_F = 0.0$ approach unity as β_0 becomes small. Beginning with these curves for $l_0/R_F = 0.0$ and proceeding to larger l_0/R_F, we see that the curves at first rise on the left sides of Figs. 4a,b,c, with curves for $l_0/R_F = 0.4$ attaining the greatest values, and curves for yet larger l_0/R_F thereafter decreasing with increasing rapidity as l_0/R_F decreases. For weak scintillation, this same type of progression is shown as a function of l_0/R_F in Refs. 1, 26, 82, 51, 28, 30, 31, 60. From Figs. 4a,b,c, we see that for the smallest β_0 (i.e., weak scintillation limit), the curves change most rapidly for larger l_0/R_F, which implies greater sensitivity for retrieval of l_0, and we see that for l_0/R_F less than about 0.80, we can obtain two values of l_0 for a given value of any of the three ratios. This is well known[26,30] because this behavior of the curves in Fig. 4b gives the usual method for retrieval of l_0 using scintillometers similar to that devised by Ochs and Hill.[26]

For $\beta_0 > 1$, Figs. 4a,b,c show many curves overlapping. This means that a measurement of any of the three ratios is insensitive to l_0/R_F and that multiple values of l_0 can be retrieved. In the retrieval of C_n^2 and l_0, the measured variance from the large-aperture scintillometer gives an approximate value of β_0 and the measured ratio then gives one or more possible values of l_0/R_F; an iteration gives the final values of C_n^2 and l_0. Since so many curves are overlapping at $\beta_0 > 1$, one obtains inaccurate values of l_0 and possibly more than two values. Hill *et al.*[82] showed this effect in their tables of errors of retrieved values of C_n^2 and l_0 for given measurement errors.

For $\beta_0 \geq 3$, Fig. 6 of Flatté *et al.*[35] shows that σ_I^2/β_0^2 will once again have an orderly behavior as l_0/R_F varies. Thus, as discussed by Hill,[1] one can, in principle, obtain l_0 from measurements of σ_I^2 for $\beta_0 > 3$.

The range $1 \leq \beta_0 \leq 3$ is problematic. The three statistics, σ_I^2, $\sigma_{\ln I}^2$, and $< \ln I >$, obtain their values from different portions of the PDF of irradiance. That all three ratios in Figs. 4a,b,c are insensitive to changes in l_0/R_F for $1 < \beta_0 < 3$ shows that the PDF of irradiance is insensitive to changes in l_0/R_F. Thus, there is probably no irradiance statistic that will be useful for retrieval of l_0 in the range $1 \leq \beta_0 \leq 3$.

Comparing Figs. 4a,b,c for $\beta_0 < 1$, we see that as β_0 increases, the curves for $\sigma^2_{\ln I}/\beta_0^2$ maintain the greatest and most regular spacing. Were it not for other considerations, this suggests that measuring $\sigma^2_{\ln I}$ is superior to measuring σ^2_I or $< \ln I >$ for purposes of retrieving inner scale. However, we must consider signal-to-noise ratio, dynamic range, etc.

Measuring irradiance using a linear amplifier has the advantage that noise and background signal can be subtracted before computing σ^2_I, provided that one designs the means of stopping the laser radiation such that noise plus background are measured. To produce the required dynamic range for a linear detector, two channels are needed: one with a gain of approximately 100, which would be suitable for $\sigma^2_I < 1$, and another with no gain for $\sigma^2_I > 1$. The rms additive noise of the detectors should be less than 10% of the average signal. For large values of σ^2_I, amplifier saturation[83-85] and insufficient number of independent samples[86-89] must be considered. Ochs and Fritz[90] gave a measurement method for overcoming the latter problem without causing great increases of averaging times, although this method is cumbersome.

Fewer independent samples are needed to measure $\sigma^2_{\ln I}$ and $< \ln I >$, and logarithmic amplifiers having sufficient dynamic range are available. However, subtraction of noise and background is not possible, and $\sigma^2_{\ln I}$ and $< \ln I >$ are more sensitive to noise than is σ^2_I. The effect of noise during a deep fade of irradiance can be a negative voltage input to the logamplifier; this produces a very erroneous output. As turbulence strength increases, the probability of occurrence of deep fades increases rapidly. In fact, this probability increases far more rapidly than is estimated on the basis of the lognormal PDF of irradiance. This is because Flatté *et al.*[36] have shown for the case of plane waves that for $\beta_0^2 \geq 0.5$ the probability of deep irradiance fades is much closer to an exponential PDF than a lognormal PDF and that the probability of deep fades of irradiance substantially exceeds the lognormal PDF even for β_0^2 as small as 0.01. We presume that similar results hold for initially spherical waves. Since $< \ln I >$ is even more sensitive to deep fades than is $\sigma^2_{\ln I}$ and since Figs. 4b and 4c show no significant advantage of $< \ln I >$ over $\sigma^2_{\ln I}$ for retrieval of inner scale, one prefers $\sigma^2_{\ln I}$ to $< \ln I >$ for obtaining inner scale.

For the case $\beta_0^2 > 0.5$, the PDFs calculated by Flatté *et al.*[36] show a remarkable regularity for deep fades. In effect, for $\beta_0^2 > 0.5$, the PDF for deep fades is approximately determined by only two parameters: $\sigma^2_{\ln I}$ and $< \ln I >$. If this result also holds for initially spherical waves, then one could design a data acquisition program to truncate the digitization for signals beyond the range of the logarithmic amplifier to obtain initial estimates of $< \ln I >$ and $\sigma^2_{\ln I}$. These estimates and knowledge of the PDF at deep fades could be used to correct $\sigma^2_{\ln I}$ for the truncation. However, much work remains to establish the PDF with adequate accuracy. At present, it is safest to retrieve inner scale from σ_I^2 using noise-and-background subtraction and variable amplifier gains.

Some motivations for studying the statistics σ_I^2, $\sigma^2_{\ln I}$, and $< \ln I >$ are that these quantities have been predicted for weak scintillation on the basis of the method of smooth perturbations, and that σ_I^2 can, in principle, be determined for all levels of scintillation from the fourth-moment equations, and that the heuristic theory was a possible candidate for predicting $\sigma^2_{\ln I}$ for all levels of scintillation. However, numerical simulation can determine the PDF of I and, hence, determine the average of any function of I; σ_I^2, $\sigma^2_{\ln I}$, and $< \ln I >$ are only three examples. An instrument designer can choose a measured quantity taking into account the instrument's hardware and software limitations. One example of such a designer quantity is the PDF truncated at irradiances beyond which the measurement is faulty.

5. Conclusion

We have performed numerical simulation of a diverged wave propagating through homogeneous atmospheric turbulence to investigate the efficacy of the statistics σ_I^2, $\sigma^2_{\ln I}$, and $< \ln I >$ for measuring inner scale. We show that the onset of strong scintillation causes these statistics to exceed the predictions of weak-scintillation theory, with the exception of

$\sigma^2_{\ln I}$ for cases of very large inner scales. We find that σ^2_I is the most advantageous statistic given present limitations, but that further study might make other quantities more useful. Measuring inner scale using scintillation is problematic for $1 < \beta_0^2 < 3$.

ACKNOWLEDGMENTS

This work was partially supported by the National Science Foundation, the Army Research Office, and the National Aeronautics and Space Administration, Marshall Space Flight Center under Research Grant NAG8-253 (Michael J. Kavaya, Technical Officer). We are grateful to S. M. Flatté for providing the simulation results of Ref. 35.

References

1. R. J. Hill, "Review of optical scintillation methods of measuring the refractive-index spectrum, inner scale and surface fluxes," Waves Random Media **2**, 179-201 (1992).

2. A. S. Gurvich and B.N. Meleshkin, "Determining the microscale of turbulence from light intensity fluctuations," Izv. Akad Nauk SSSR. Fiz. Atmos. Okeana **2**, 688-694 (1966). English, Izv. Atmosph. Oceanic Phys. **2**, 417-420 (1966).

3. P. M. Livingston, "Proposed method of inner scale measurement in a turbulent atmosphere," Appl. Opt. **11**, 684-687 (1972).

4. N. Ts. Gomboyev, E. V. Zubritskiy, G. F. Malygina, V. L. Mironov, and S. S. Khmelevtsov, "Determination of internal scale of turbulence from optical measurements," Proc. of the Third All-Union Symposium on Propagation of Laser Radiation in the Atmosphere, (Tomsk: Institute of Atmospheric Optics), 183-184 (1975). (Engl. Trans. available from National Translation Center, Library of Congress, Washington, DC 20540, USA).

5. A. F. Zhukov, I. V. Lukin, and R. Sh. Tsvyk, "Amplitude measurements of inner scale of turbulence," Proc. of the All-Union Symposium on Laser and Acoustic Monitoring of the Atmosphere, Part II (Tomsk: Institute of Atmospheric Optics), 29-32 (1984). (Engl. Trans. available from National Translation Center, Library of Congress, Washington, DC 20540, USA).

6. Ye. A. Monastyrnyy, G. Ya Patrushev, A. I. Petrov, and V. V. Pokasov, "Method for determining the inner scale of turbulence," Proc. of the All-Union Symposium on Laser and Acoustic Monitoring of the Atmosphere, Part II (Tomsk: Institute of Atmospheric Optics), 26-28 (1984). (Engl. Trans. available from National Translation Center, Library of Congress, Washington, DC 20540, USA).

7. A. V. Artem'ev and A.S. Gurvich, "Experimental study of coherence-function spec-

tra," Izv. Vysh. Ucheb. Zaved. Radiofiz. **14**, 734-738 (1971). English. Radiophys. and Quantum Electron. **14**, 580-583, (1971).

8. W. A. Coles and R.G. Frehlich, "Simultaneous measurements of angular scattering and intensity scintillations in the atmosphere," J. Opt. Soc. Am. **72**, 1041-1048 (1982).

9. J. W. Strohbehn, "The feasibility of laser experiments for measuring the permittivity spectrum of the turbulent atmosphere," J. Geophys. Res. **75**, 1067-10766 (1970).

10. V. P. Lukin, V. L. Mironov, V.V. Pokasov, and S.S. Khmelevtsov, "Optical phase measurements of refractive-index fluctuations," Izv. Akad Nauk SSSR. Fiz. Atmos. Okeana **12**, 550-553 (1976). English. Izv. Atmosph. Oceanic Phys. **12**, 333-335, (1976).

11. A. Consortini and L. Ronchi, "Laser propagation through atmospheric turbulence," Alta Frequenza **10**, 769-772 (1974).

12. A. Consortini, "Measurements of the angle of arrival fluctuations of a laser beam due to turbulence," AGARD Conf. Proc. No. 183, Optical Propagation in the Atmosphere (National Technical Information Service, 5285 Port Royal Rd., Springfield, VA 22161, 1976).

13. A. Consortini, P. Pandolfini, C. Romanelli, and R. Vanni, "Turbulence investigation of small scale by angle-of-arrival fluctuations of a laser beam," Optica Acta **27**, 1221-1228 (1980).

14. A. Consortini, K. A. O'Donnell, and G. Conforti, "Determination of the inner scale of atmospheric turbulence through laser beam wander," Proc. of the 14th Congress of the International Commission for Optics (Quebec, August 1987) SPIE Conf. Proc. **813**, 117 (1987).

15. A. Consortini, "Role of the inner scale of atmospheric turbulence in optical propagation and methods to measure it," Scattering in Volumes and Surfaces ed. M. Nieto-Vesperinas and J. C. Dainty (New York: Elsevier), 73-90, (1990).

16. A. Consortini, Y. Y. Sun, L. Z. Ping, and G. Conforti, "A mixed method for measuring the inner scale of atmospheric turbulence," J. Mod. Opt. **37**, 1555-1560 (1990).

17. A. Consortini and K. A. O'Donnell, "Beam wandering of thin parallel beams through atmospheric turbulence," Waves in Random Media **3**, S11-28 (1991).

18. R. G. Frehlich, "Variance of focal-plane centroids," J. Opt. Soc. Am. A **7**, 2119-2140 (1990).

19. D. A. Gray and A.T. Waterman, Jr., "Measurement of fine-scale atmospheric structure using an optical propagation technique," J. Geophys. Res. **75**, 1077-1083 (1970).

20. R. G. Frehlich, "Estimation of the parameters of the atmospheric turbulence spectrum using measurements of the spatial intensity covariance," Appl. Opt. **27**, 2194-2198 (1988).

21. R. Frehlich, "Laser scintillation measurements of the temperature spectrum in the atmospheric surface layer," J. Atmos. Sci. **49**, 1494-1509 (1992).

22. A. S. Gurvich, "The determination of turbulence characteristics from light scattering experiments," Atmos. Oceanic Phys. **4**, 90-95 (1968).

23. N. S. Time, "Estimation of the turbulence spectrum in the dissipation range from measurements of laser light fluctuations," Atmos. Oceanic Phys. **8**, 48-49 (1972).

24. R. J. Hill, "Theory of measuring the path-averaged inner scale of turbulence by spatial filtering of optical scintillation," Appl. Opt. **21**, 1201-1211 (1982).

25. R. J. Hill and G.R. Ochs, "Fine calibration of large-aperture optical scintillometers and an optical estimate of the inner scale of turbulence," Appl. Opt. **17**, 3608-3612 (1978).

26. G. R. Ochs and R. J. Hill, "Optical-scintillation method of measuring turbulence inner scale," Appl. Opt. **24**, 2430-2432 (1985).

27. Z. Azar, E. Azoulay, and M. Tur, "Optical bichromatic correlation method for the

remote sensing of inner scale," Technical Digest, Conf. on Laser and Electro-Optics, MA4 (Washington, DC: Optical Society of America) (1987).

28. E. Azoulay, V. Thiermann, A. Jetter, A. Kohnle, and Z. Azar, "Optical measurements of the inner scale of turbulence," J. Phys. D: Appl. Phys. **21**, 541-544 (1988).

29. V. Thiermann and E. Azoulay, "A two wavelength laser scintillometer for monitoring surface layer fluxes under near neutral conditions," Proc. of the International Laser Radar Conf. (Innichen-San Candido, June 1988) 70-73 (1988).

30. R. J. Hill, "Comparison of scintillation methods for measuring the inner scale of turbulence," Appl. Opt. **27**, 2187-2193 (1988).

31. V. Thiermann and H. Grassl, "The measurement of turbulent surface-layer fluxes by use bichromatic scintillation," Boundary-Layer Meteorology **58**, 367-389 (1992).

32. R. G. Frehlich and G. R. Ochs, "Effects of saturation on the optical scintillometer," Appl. Opt. **29**, 548-553 (1990).

33. T. Wang, G.R. Ochs, and S.F. Clifford, "A saturation-resistant optical scintillometer to measure C_n^2," J. Opt. Soc. Am. **68**, 334-338 (1978).

34. M. I. Charnotskii, "Asymptotic analysis of the flux fluctuations averaging and finite-size source scintillations in a random medium," Waves Random Media **1**, 223-243 (1991).

35. S. M. Flatté, G. Wang, and J. Martin, "Irradiance variance of optical waves through atmospheric turbulence by numerical simulation and comparison with experiment," J. Opt. Soc. Am. A **10**, 2363-2370 (1993).

36. S. M. Flatté, C. Brasher, G. Wang, "Probability-density functions of irradiance for waves in atmospheric turbulence calculated by numerical simulation," J. Opt. Soc. Am. A **11**, 2080-2092 (1994).

37. J. A. Fleck, Jr., J. R. Morris, and M. D. Feit, "Time-dependent propagation of high

energy laser beams through the atmosphere," Appl. Phys., **10**, 129-160 (1976).

38. J. M. Martin and S. M. Flatté, "Intensity images and statistics from numerical simulation of wave propagation in 3-D random media," Appl. Opt. **27**, 2111-2126 (1988).

39. J. M. Martin and Stanley M. Flatté, "Simulation of point-source scintillation through three-dimensional random media," J. Opt. Soc. Am. A **7**, 838-847 (1990).

40. J. Martin, "Simulation of wave propagation in random media: theory and applications," in *Wave Propagation in Random Media (Scintillation)* Editors: V. I. Tatarskii, A. Ishimaru, and V. U. Zavorotny, SPIE Press and IOP Publishing (1993).

41. C. A. Davis and D. L. Walters, "Atmospheric inner-scale effects on normalized irradiance variance," Appl. Opt. **33**, 8406-8411 (1994).

42. Wm. A. Coles, J. P. Filice, R. G. Frehlich, and M. Yadlowsky, "Simulation of wave propagation in three-dimensional random media," Appl. Opt. **34**, 2089-2101 (1995).

43. A. Consortini, F. Cochetti, J. H. Churnside, and R. J. Hill, "Inner-scale effect on irradiance variance measured for weak-to-strong atmospheric scintillation," J. Opt. Soc. Am. A **10**, 2354-2362 (1993).

44. V. I. Tatarskii, "Light propagation in a medium with random refractive index inhomogeneities in the Markov random process approximation," Zh. Eksp. Teor. Fiz. **56**, 2106-2117 (1969). English, Sov. Phys. JETP **29**, 1133-1138 (1969).

45. V. I. Klyatskin and V.I. Tatarskii, "The parabolic equation approximation for propagation of waves in a medium with random inhomogeneities," Zh. Eksp. Teor. Fiz. **58**, 624-634 (1970). English, Sov. Phys. JETP **31**, 335-339 (1970).

46. V. I. Klyatskin and V. I. Tatarskii, "A new method of successive approximations in the problem of the propagation of waves in a medium having random large-scale inhomogeneities" Izv. Vysh. Ucheb. Zaved. Radiofiz. **14**, 1400-1415 (1971). English, Radiophys.

and Quantum Electron. **14**, 1100-1111 (1971).

47. V. I. Klyatskin, "Applicability of the approximation of a Markov random process in problems relating to the propagation of light in a medium with random inhomogeneities," Zh. Eksp. Teor. Fiz. **57**, 952-958 (1969). English, Sov. Phys. JETP. **30**, 520-523 (1970).

48. V. U. Zavorotnyi, "Strong fluctuations of electromagnetic waves in a random medium with finite longitudinal correlation of the inhomogeneities," Zh. Eksp. Teor. Fiz. **75**, 56-65 (1978). English, Sov. Phys. JETP **48,** 27-31 (1978).

49. A. M. Obukhov, "The structure of the temperature field in turbulent flow," Izv. Akad. Nauk SSSR, Ser. Geogr. i Geofiz. **13**, 58-69 (1949).

50. V. I. Tatarskii, "The Effects of the Turbulent Atmosphere on Wave Propagation", Keter Press, Jerusalem (1971).

51. R. J. Hill and S.F. Clifford, "Modified spectrum of atmospheric temperature fluctuations and its application to optical propagation," J. Opt. Soc. Am. **68**, 892-899 (1978)

52. R. J. Hill, "Models of the scalar spectrum for turbulent advection, "J. Fluid Mech. **88**, 541-562 (1978).

53. L. Mahrt, "Intermittency of atmospheric turbulence," J. Atmos. Sci. **46,** 79-95 (1989)

54. R. J. Hill, "Effects of large-scale intermittency of turbulence on scalar spectra at high wave numbers. NOAA Tech. Memo. ERL 409-WPL 54 (National Technical Information Service, 5285 Port Royal Rd., Springfield, VA 22161, 1980).

55. J. H. Churnside and R. G. Frehlich, "Experimental evaluation of log-normally modulated Rician and IK models of optical scintillation in the atmosphere," J. Opt. Soc. Am. A **6**, 1760-1766 (1989).

56. J. Gozani, "Wave propagation in an intermittent quasi-homogeneous turbulent

medium," Opt. Lett. **17**, 559-561 (1992).

57. R. G. Frehlich, "The effects of global intermittency on wave propagation in random media," Appl. Opt. **33**, 5764-5769 (1994).

58. V. I. Tatarskii and V.U. Zavorotnyi, "Wave propagation in random media with fluctuating turbulent parameters," J. Opt. Soc. Am. A **2**, 2069-2076 (1985)

59. V. I. Tatarskii, "Some new aspects in the problem of waves and turbulence," Radio Sci. **22**, 859-865 (1987).

60. R. J. Hill and G. R. Ochs, "Inner-scale dependence of scintillation variances measured in weak scintillation," J. Opt. Soc. Am. A **9**, 1406-1411 (1992).

61. R. S. Lawrence and J. W. Strohbehn, "A survey of clear air propagation effects relevant to optical communications," Proc. IEEE **58**, 1523-1545 (1970).

62. M. E. Gracheva, A.S. Gurvich, S.S. Kashkarov, and V. V. Pokasov, "Similarity relations for strong fluctuations of light in a turbulent medium," Zh. Eksp. Teor. Fiz. **67**, 2035-2046 (1974). English, Sov. Phys. JETP **40**, 1011-1016 (1974).

63. A. S. Gurvich and V.I. Tatarskii, "Coherence and intensity fluctuations of light in the turbulent atmosphere," Radio Sci. **10**, 3-14 (1975).

64. A. S. Gurvich, M.A. Kallistratova, and F. E. Martvel', "An investigation of strong fluctuations of light intensity in a turbulent medium at a small wave parameter," Izv. Vysh. Ucheb. Zaved. Radiofiz. **20**, 1020-1031 (1977). English, Radiophys. and Quantum Electron. **20**, 705-714 (1977).

65. R. J. Hill, "Optical propagation in turbulent water," J. Opt. Soc. Am. **68**, 1067-1072 (1978).

66. R. A. Elliot, J. R. Kerr, and P. A. Pincus, "Optical propagation in laboratory-generated turbulence," Appl. Opt. **18**, 3315-3323 (1979).

67. C. G. Little, "A diffraction theory of the scintillation of stars on optical and radio wave-lengths," Mon. Not. R. Astr. Soc. **111**, 289-302 (1951).

68. K. S. Gochelashvily, V.G. Pevgov, and V.I. Shishov, "Saturation of fluctuations of the intensity of laser radiation at large distances in a turbulent atmosphere (Fraunhofer zone of transmitter)" Kvant. Elektron. **1**, 1156-1165 (1974). English, Sov. J. Quant. Electron. **4**, 632-637 (1974).

69. A. M. Prokhorov, F.V.Bunkin, K.S. Gochelashvily, and V.I. Shishov, "Laser irradiance propagation in turbulent media," Proc. IEEE **63,** 790-811 (1975).

70. I. G. Yakushkin, "Asymptotic calculations of field-intensity fluctuations in a turbulent medium for long paths," Izv. Vysh. Ucheb. Zaved., Radiofiz. **18**, 1660-1666 (1975). English, Radiophys. and Quantum Electron. **18**, 1224-1229 (1975).

71. V. U. Zavorotnyi, V.I. Klyatskin, and V.I. Tatarskii, "Strong fluctuations of the intensity of electromagnetic waves in randomly inhomogeneous media," Zh. Eksp. Teor. Fiz. **73**, 181-197 (1977). English, Sov. Phys. JETP **46**, 252-260 (1977).

72. M. Tur, "Numerical solutions for the fourth moment of a plane wave propagating in a random medium," J. Opt. Soc. Am. **72**, 1683-1691 (1982).

73. R. J. Hill and S.F. Clifford, "Theory of saturation of optical scintillation by strong turbulence for arbitrary refractive-index spectra," J. Opt. Soc. Am. **71**, 675-685 (1981).

74. S. F. Clifford, G.R. Ochs, and R.S. Lawrence, "Saturation of optical scintillation by strong turbulence," J. Opt. Soc. Am. **64**, 148-154 (1974).

75. R. J. Hill, "Theory of saturation of optical scintillation by strong turbulence: plane-wave variance and covariance and spherical-wave covariance," J. Opt. Soc. Am. **72**, 212-221 (1982).

76. R. G. Frehlich, S. M. Wandzura, and R. J. Hill "Log-amplitude covariance for waves

propagating through very strong turbulence" J. Opt. Soc. Am. A **4**, 2158-2161 (1987).

77. G. R. Ochs, "Measurements of 0.63μ m laser-beam scintillation in strong atmospheric turbulence," ESSA Tech. Rep. ERL 154-WPL 10 (National Technical Information Service, 5285 Port Royal Rd., Springfield, VA 22161, 1969).

78. G. Parry and P.N. Pusey, "K distributions in atmospheric propagation of laser light," J. Opt. Soc. Am. **69**, 796-798 (1979).

79. G. Parry, "Measurements of atmospheric turbulence induced intensity fluctuations in a laser beam, Optica Acta **28**, 715-728 (1981).

80. R. L. Phillips and L.C. Andrews, "Measured statistics of laser-light scattering in atmospheric turbulence," J. Opt. Soc. Am. **71**, 1440-1445 (1981).

81. R. J. Hill and J. H. Churnside, "Observational challenges of strong scintillations of irradiance," J. Opt. Soc. Am. A **5**, 445-447 (1988).

82. R. J. Hill, W. D. Otto, and J. R. Jordan, "Operation of the fluxes scintillometer," NOAA Tech. Memo. ERL ETL-241 (National Technical Information Service, 5285 Port Royal Rd., Springfield, VA 22161, 1994).

83. A. Consortini and G. Conforti, "Detector saturation effect on higher-order moments of intensity fluctuations in atmospheric laser propagation measurements," J. Opt. Soc. Am. A **1**, 1075-1077 (1984).

84. A. Consortini, E. Briccolani, and G. Conforti, "Strong-scintillation-statistics deterioration due to detector saturation," J. Opt. Soc. Am. A **3**, 101-107 (1986).

85. A. Consortini and R. J. Hill, "Reduction of the moments of intensity fluctuations caused by amplifier saturation for both the K and log-normally modulated exponential probability densities," Opt. Lett. **12**, 304-306 (1987).

86. J. H. Churnside and R. J. Hill, "Probability density of irradiance for strong path-

integrated refractive turbulence," J. Opt. Soc. Am. A **4,** 727-733 (1987).

87. N. Ben-Yosef and E. Goldner, "Sample size influence on optical scintillation analysis. 1: Analytical treatment of the higher-order irradiance moments," Appl. Opt. **27**, 2167-2177 (1988).

88. E. Goldner and N. Ben-Yosef, "Sample size influence on optical scintillation analysis. 2: Simulation approach," Appl. Opt. **27**, 2172-2177 (1988).

89. R. G. Frehlich and James H. Churnside,"Statistical properties of estimates of the moments of laser scintillation," J. Mod. Opt. **36**, 1645-1659 (1989).

90. G. R. Ochs and R. B. Fritz, "Observations of spherical-wave scintillation in strong refractive-index turbulence," NOAA Tech. Memo. ERL WPL-154 (National Technical Information Service, 5285 Port Royal Rd., Springfield, VA 22161, 1988).

FIGURES

Fig. 1a. σ_I^2 is shown versus σ_{Rytov}^2. From top to bottom, the order of the curves corresponds to the values of l_0/R_F from top to bottom in the legend. The straight solid line shows $\sigma_I^2 = \sigma_{Rytov}^2$.

Fig. 1b. Similar to Fig. 1a, but showing larger values of σ_{Rytov}^2. The circles are values from Fig. 1a. The lines connect points calculated by Flatté *et al.*[35] From top to bottom, the circles and lines are in the same order as the values of l_0/R_F in the legend.

Fig. 2. $\sigma_{\ln I}^2$ versus σ_{Rytov}^2. From top to bottom along the far right edge, the order of the curves is the same as the order of the values of l_0/R_F in the legend. The straight solid line shows $\sigma_{\ln I}^2 = \sigma_{Rytov}^2$.

Fig. 3. The mean of logirradiance is shown versus σ_{Rytov}^2. From top to bottom, the order of the curves is the same as the order of the values of l_0/R_F in the legend. The solid curve shows $< \ln I >= -\sigma_{Rytov}^2/2$.

Fig. 4a. Scaled irradiance variance versus β_0. See caption of Fig. 4c.

Fig. 4b. Scaled logirradiance variance versus β_0. See caption of Fig. 4c.

Fig. 4c. Scaled mean of logirradiance versus β_0. Here, as in Figs. 4a and b, the legend gives the values of l_0/R_F from top to bottom that correspond to the curves from top to bottom on the left side of the figure.

Fig. 5. Ratio of the variance of log irradiance using the heuristic theory to the variance of log irradiance from simulations. The legend gives the values of l_0/R_F from top to bottom that correspond to the curves from top to bottom at $\sigma^2_{Rytov} = 1$.

Appendix A: Comparison with Heuristic Theory

With regard to Fig. 2, we noted that $\sigma^2_{\ln I}$ differs from the prediction of the heuristic theory originated by Clifford *et al.*[74] and refined by Hill and Clifford.[73,75] We can obtain $\sigma^2_{\ln I}$ from the heuristic theory using interpolation on the tabulated values given in Ref. 73. In Fig. 5, we show the ratio of $\sigma^2_{\ln I}$ from the heuristic theory to $\sigma^2_{\ln I}$ from our simulation. Figure 5 shows that the heuristic theory has significant error that depends on l_0/R_F. For logirradiance variance, the refined heuristic theory[73,75] has correct asymptotic limits for $\sigma^2_{Rytov} \to \infty$, as well as for $\sigma^2_{Rytov} \to 0$; only the latter limit is evident in Fig. 5. Frehlich *et al.*[76] showed that the heuristic theory predicts incorrect covariance of logirradiance in the limit $\sigma^2_{Rytov} \to \infty$, although the variance of logirradiance is correct for $\sigma^2_{Rytov} \to \infty$. Our unpublished comparisons of covariance of logirradiance measured by Ochs and Fritz[90] with those predicted by the heuristic theory produced poor agreement.

We conclude that the heuristic theory should not be used to calculate C_n^2 and l_0 from scintillation measurements. In fact, using $\sigma^2_{\ln I} \simeq \sigma^2_{Rytov}$ is more accurate than the heuristic theory, with the exception of the following computed cases: $\sigma^2_{Rytov} \geq 5$; $\sigma^2_{Rytov} = 3$ and $l_0/R_F \geq 0.5$; and $l_0/R_F = 2.5$.

Figure 1a Hill & Frehlich

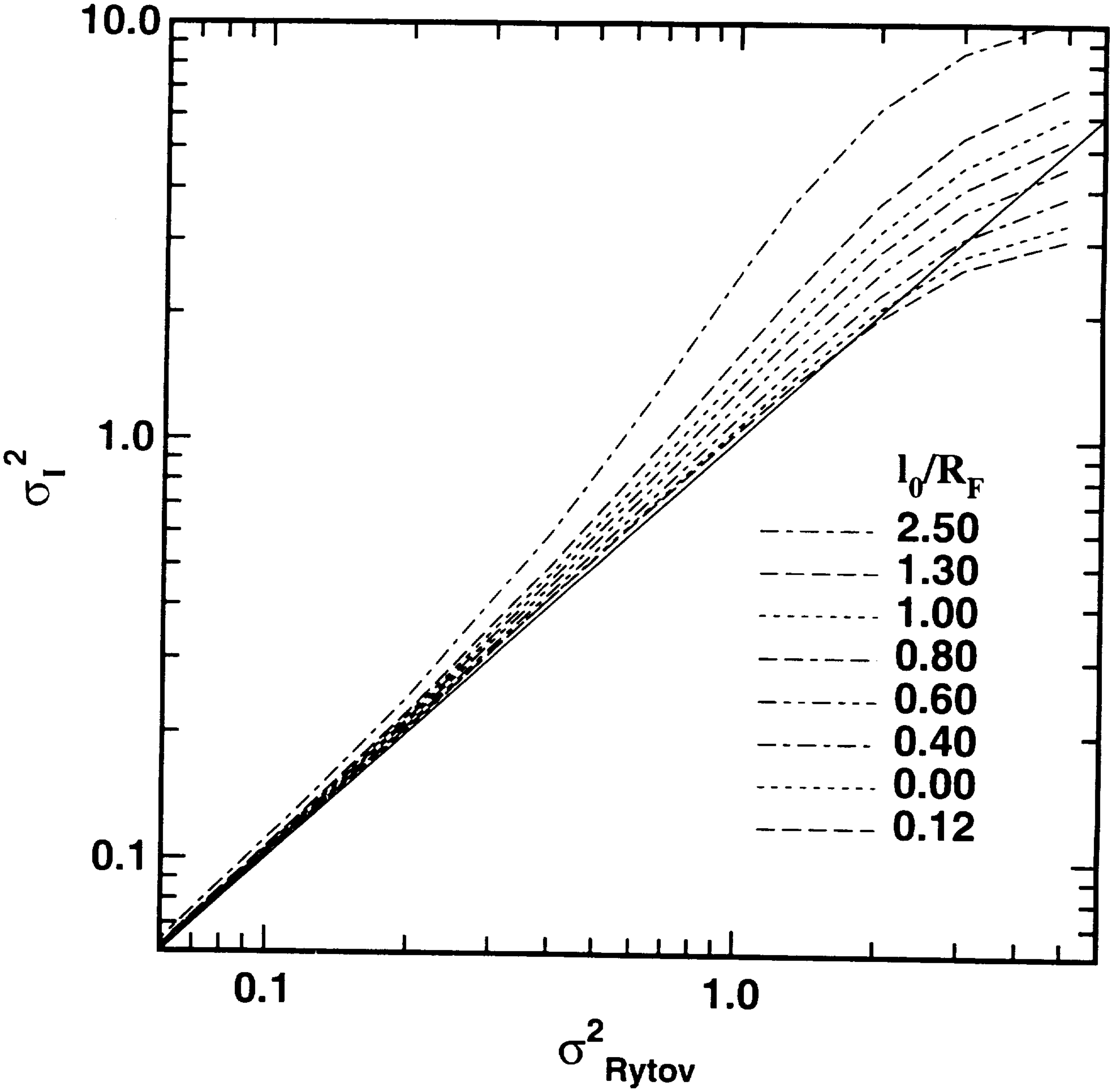

Figure 1b Hill & Frehlich

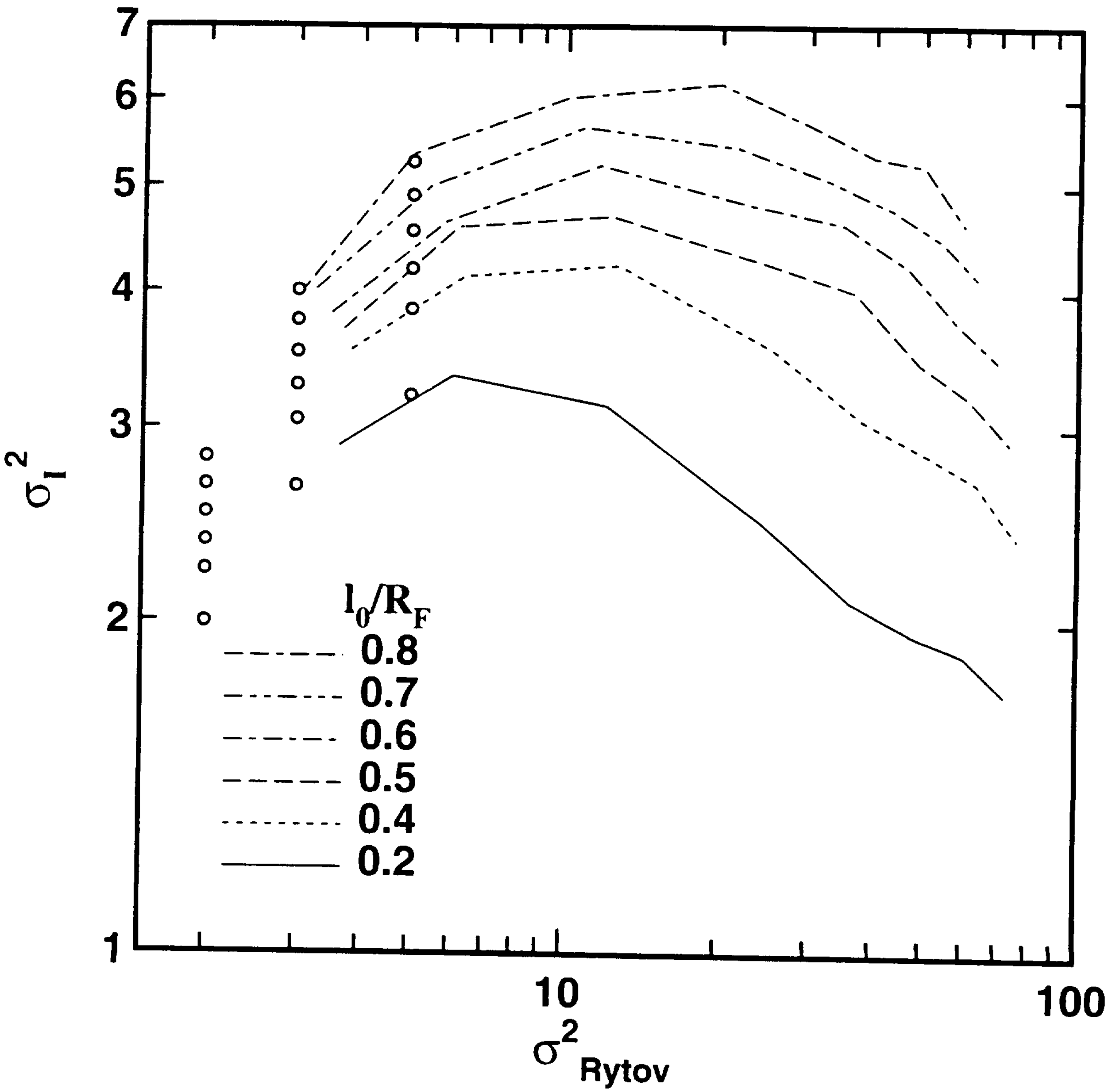

Figure 2 Hill & Frehlich

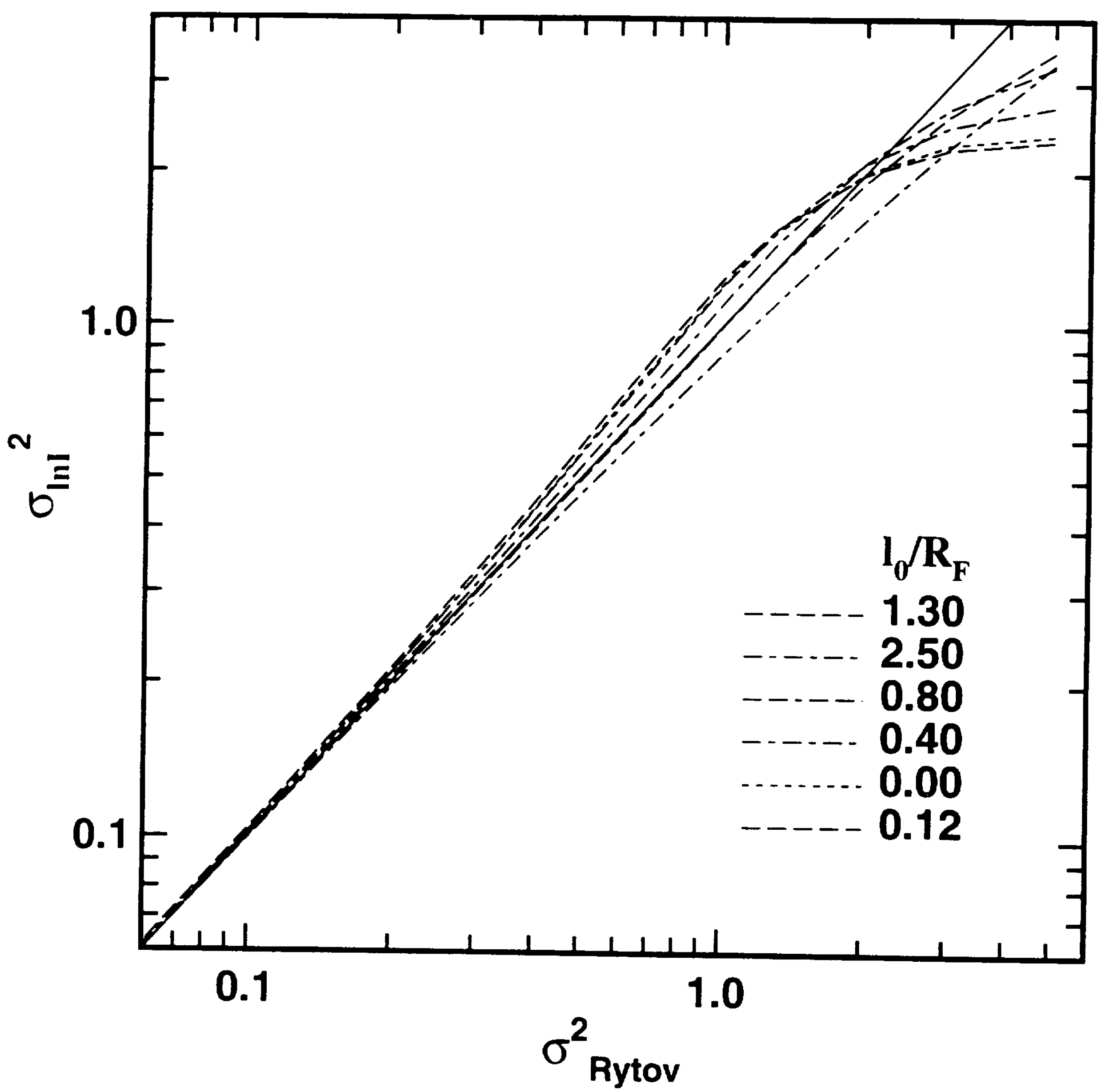

Figure 3 Hill & Frehlich

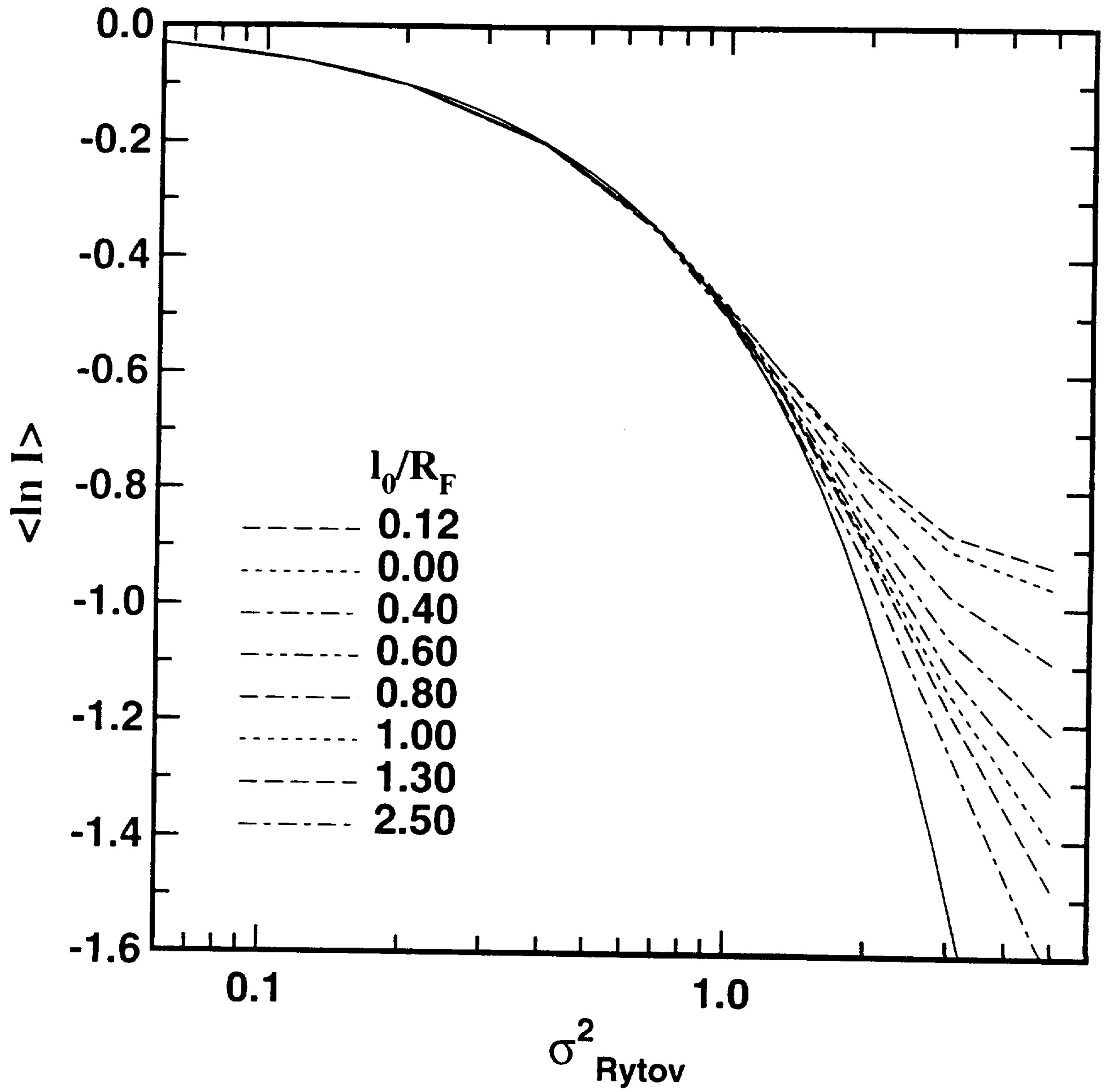

Figure 4a Hill & Frehlich

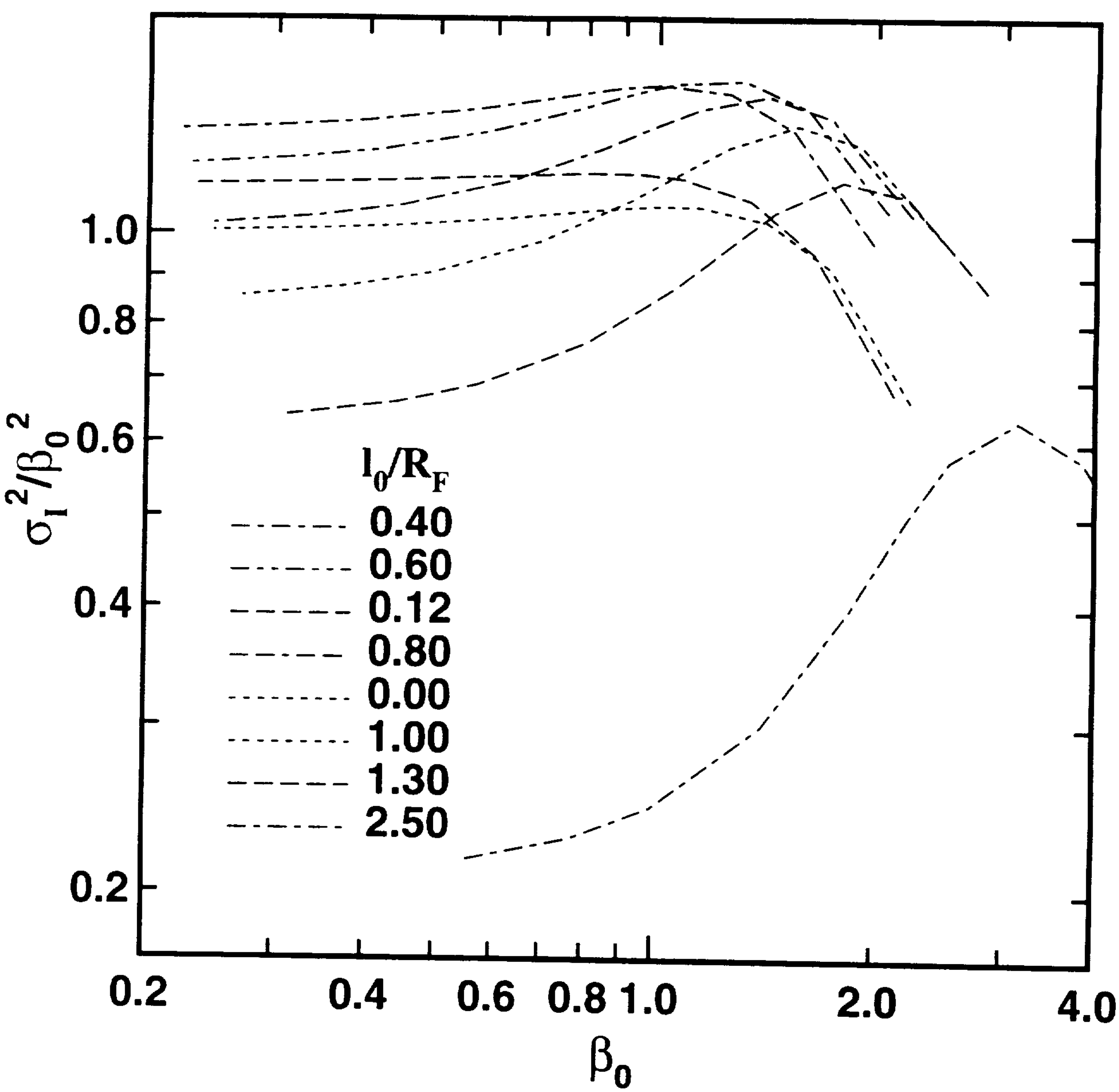

Figure 4b Hill & Frehlich

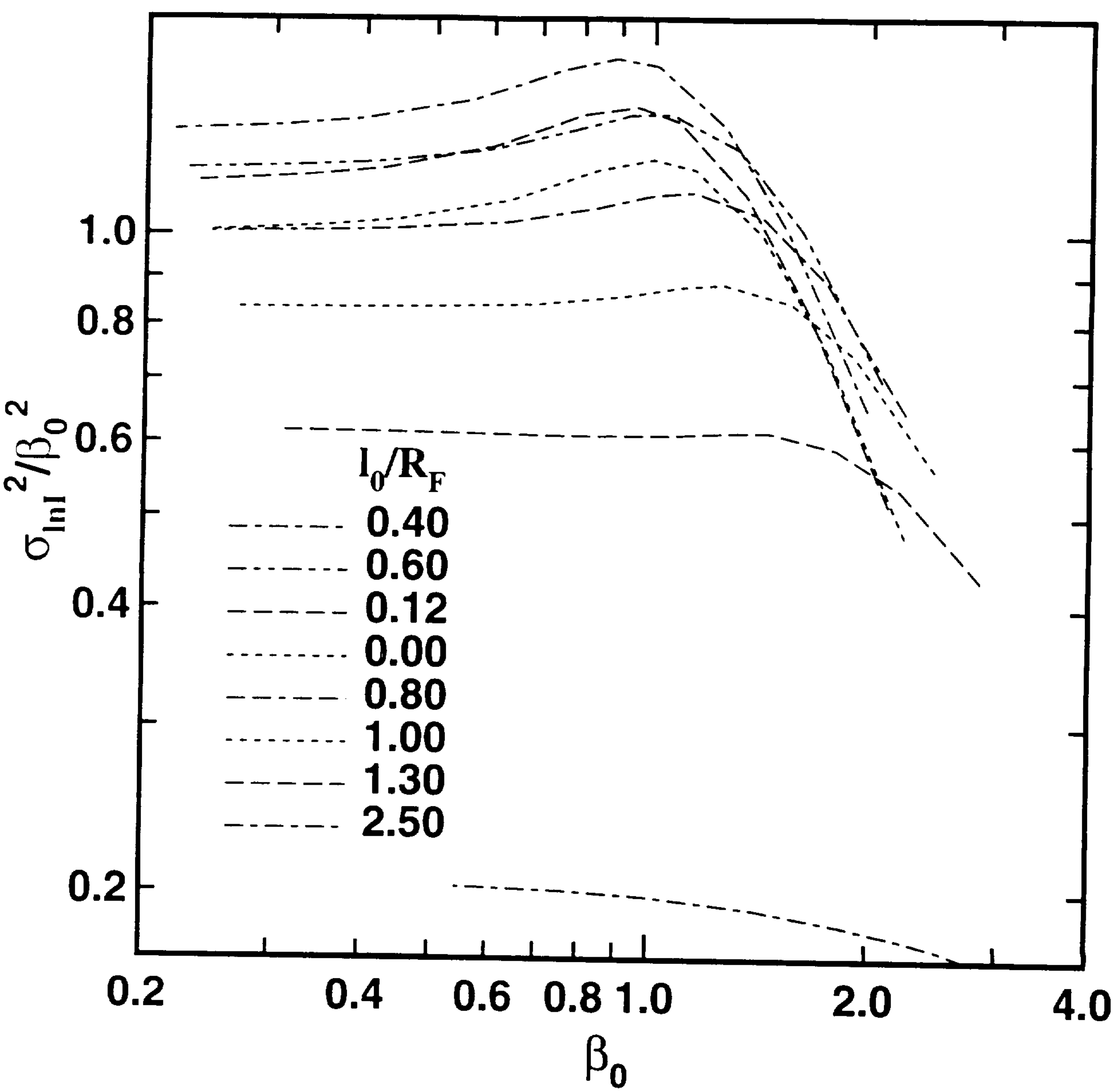

Figure 4c Hill & Frehlich